

**SAILING YACHT PERFORMANCE IN  
CALM WATER AND IN WAVES**

**J. Gerritsma, J.A. Keuning  
and A. versluis**

**Report No. 938-P**

**January 1993**

# SAILING YACHT PERFORMANCE IN CALM WATER AND IN WAVES

by

J. Gerritsma, J.A. Keuning and A. Versluis  
Ship Hydromechanics Laboratory  
Delft University of Technology  
Mekelweg 2, 2628 CD Delft, The  
Netherlands

## Summary

The Delft Systematic Yacht Hull Series has been extended to a total of 39 hull form variations, covering a wide range of length-displacement ratios and other form parameters. The total set of model-experiment results, including upright and heeled resistance as well as side-force and stability, has been analysed and polynomial expressions to approximate these quantities are presented. In view of the current interest in the performance of sailing yachts in waves, the added resistance in irregular waves of 8 widely different hull form variations has been calculated. Analysis of the results shows that the added resistance in waves strongly depends on the product of displacement-length ratio and the gyroradius of the pitching motion.

## Contents

1. Introduction
2. Velocity prediction in calm water
  - 2.1. Main dimensions and form coefficients
  - 2.2. Determination of the hydrodynamic resistance
    - 2.2.1. Upright resistance
    - 2.2.2. Induced resistance
    - 2.2.3. Resistance due to heel
  - 2.3. Side force as a function of heel and leeway
  - 2.4. Stability
3. Prediction of added resistance in waves
4. References

## Nomenclature

$A_w$	- waterline area
$A_x$	- maximum cross-section area
$AR$	- aspect ratio
$B_{WL}$	- waterline breadth
$B_{MAX}$	- maximum beam

$C_F$	- frictional resistance coefficient
$C_H$	- heeled resistance coefficient
$C_M$	- maximum cross section coefficient
$C_P$	- prismatic coefficient
$C_{Di}$	- induced resistance coefficient
$C_L$	- lift coefficient
$F_H$	- side force
$F_n$	- Froude number
$G_M$	- metacentric height
$g$	- acceleration due to gravity
$H_{1/3}$	- significant wave height
$k_{yy}$	- pitch gyroradius
$LCB$	- longitudinal center of buoyancy in % $L_{WL}$ aft of $L_{WL}/2$
$L_{WL}$	- waterline length
$M_N$	- residuary stability
$q$	- stagnation pressure - $\frac{1}{2}\rho V^2$
$R_\varphi$	- total resistance with heel and leeway
$R_T$	- total resistance in upright position
$R_F$	- frictional resistance
$R_R$	- residuary resistance
$R_i$	- induced resistance
$R_H$	- resistance due to heel
$R_{AW}$	- added resistance in waves
$S_k$	- wetted area keel
$S_c$	- wetted area canoe body
$S_r$	- wetted area rudder
$S_\zeta$	- spectral density
$\bar{T}_1$	- wave period $\bar{T}_1 = 2 \pi m_0/m_1$
$T_e$	- period of encounter
$T_E$	- effective draught
$T$	- total draught
$T_c$	- draught of canoe body
$V$	- speed
$\zeta_a$	- wave amplitude
$\varphi$	- heel angle
$\lambda$	- wave length
$\rho$	- density of water
$\omega$	- circular frequency
$\nabla_c$	- volume of displacement
$\Delta$	- weight of displacement
$\beta$	- leeway angle
$\mu_w$	- wave direction
$\nu$	- kinematic viscosity

## 1. Introduction

On the tenth Chesapeake Sailing Yacht Symposium the results of an extension of the Delft Systematic Yacht hull series has been presented.

This Series II consists of 6 medium- to light displacement-length hull forms in view of the trend towards lighter sailing yachts which have a greater speed potential, in particular in reaching conditions.

The Series has been extended and completed with model tests of an additional Series of 11 hull form variations: Series III.

The total Series now consists of thirty nine models.

Series III has been added to increase the reliability of the upright resistance prediction for light displacement yachts, in particular in the high speed range with  $F_n > 0.45$  [1].

The need for the extension of the Series with the light-displacement hull forms can be illustrated by a comparison of the predicted upright resistance for model 25 according to the expression as used by the IMS and by the new Delft formulation versus the experimental result, see Figure 1 [2].

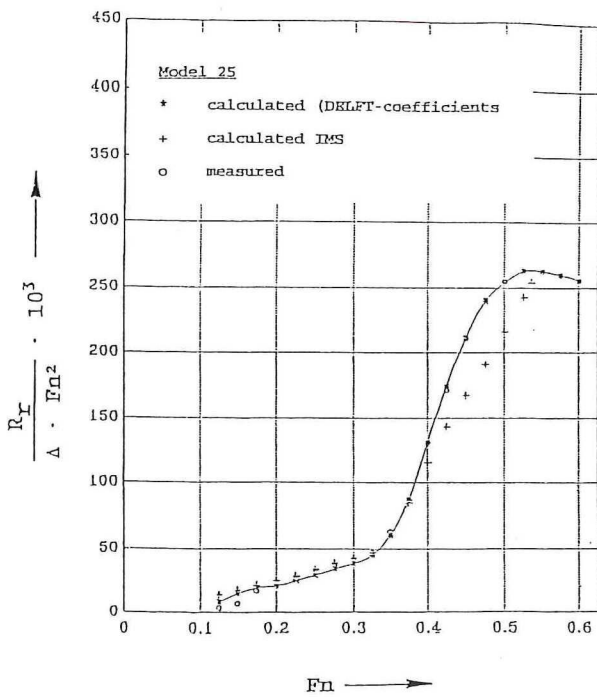


Fig. 1: Comparison of IMS and Delft approximations of the residuary resistance with experiments [2].

Another aspect of light displacement hull forms is the sailcarrying capacity. Light sailing yachts with a large  $B_{WL}/T_c$  ratio loose 20 to 30 % stability at high speed compared with the result of a hydrostatic stability calculation. This seems to be caused by more extreme distortion of the free surface when heeled at high speeds. Neglecting these effects could lead to erroneous velocity predictions.

Therefore the systematic Series results also have been used to reanalyse the forward speed effects on stability for

all considered hull form variations.

The upright resistance, the heeled resistance, the sideforce and the stability could be expressed in simple hull form parameters:

$$L_{WL}/v_c^{1/3}, B_{WL}/T_c, T_c/T, L_{WL}/B_{WL}, \\ A_w/v_c^{2/3}, LCB, C_p \text{ at constant } v/\sqrt{gL_{WL}}$$

In general, velocity predictions of sailing yachts concern the calm water performance.

However the influence of seawaves on the resistance can be very substantial, in particular when resonance conditions for the pitching motion are encountered. Also in this respect, light-displacement yachts differ from medium- and heavy-displacement yachts because the natural periods of pitch and heave will be smaller. Consequently, resonance conditions will occur in a different part of the wave spectrum resulting, in many cases, in lower added resistance for the light displacement yacht, in comparison with a larger displacement yacht with comparable main dimensions.

The total resistance, including this added resistance, could be taken into account in a performance calculation, when the relative merits of yachts in a seaway have to be compared, for instance in the case of race handicapping.

In this paper the possibilities to include such an added resistance in waves calculation are discussed, also with regard to the use of the systematic hull form variations of the Delft Series in this respect.

## 2. Velocity prediction in calm water

In 1977 the results of model experiments with 9 systematic variations of sailing yacht hull forms were published [5]. The measurements included the determination of the upright resistance, the heeled and induced resistance, the sideforce and the stability.

An extension of this research with another series of 12 hull forms was presented in 1981 [6].

All of the 22 hull form variations were based on the sailing yacht Standfast 43 designed by Frans Maas. (Series I).

In view of the trend towards light-displacements a further extension of the series with 6 models (Series II) was completed providing the same kind of information as for Series I and published in 1988 [7] and 1991 [8]. These hull form variations were based on a van de Stadt & Partners designed parent form. Finally a third series (Series III) of eleven models has been tested, but only in the upright condition, without leeway.

The speed range for Series I is limited to  $F_n = 0.45$ , but for the Series II and III speeds corresponding to  $F_n = 0.75$

have been included. With the parent model of Series I three modifications of the keel span have been tested.

### 2.1. Main dimensions and form coefficients

The main dimensions of the models 1-39, extrapolated to a waterline length  $L_{WL} = 10$  meters are given in Table 2, whereas in Table 3 the form coefficients and the longitudinal position of the center of buoyancy are summarized.

In Table 1 the ranges of some ratio's of main dimensions and form coefficients are given.

Table 1

Ranges of hull form parameters	
$L_{WL}/B_{WL}$	: 2.76 - 5.00
$B_{WL}/T_c$	: 2.46 - 19.32
$L_{WL}/v_c^{1/3}$	: 4.34 - 8.50
LCB	: 0.0 - -6.0%
$C_p$	: 0.52 - 0.60

Table 2  
Main dimensions

model no.	$L_{WL}$ m	$B_{max}$ m	$B_{WL}$ m	$T_c$ m	T m	$v_c$ $m^3$	$S_c$ $m^2$	$\lambda_X$ $m^2$	$\lambda_W$ $m^2$
1	10.04	3.67	3.17	0.794	2.16	9.18	25.4	1.62	21.8
2	10.04	3.21	2.76	0.907	2.28	9.18	23.9	1.62	19.1
3	10.06	4.25	3.64	0.681	2.05	9.16	27.6	1.63	25.2
4	10.06	3.32	2.05	0.722	2.09	7.55	23.0	1.34	19.8
5	10.05	4.24	3.64	0.920	2.29	12.10	29.1	2.15	25.3
6	10.00	3.66	3.17	1.064	2.43	12.24	27.5	2.16	21.9
7	10.06	3.68	3.17	0.640	2.01	7.35	24.1	1.31	21.8
8	10.15	3.54	3.05	0.794	2.16	9.18	25.4	1.57	22.1
9	10.07	3.81	3.28	0.794	2.16	9.18	25.0	1.68	21.5
10	10.00	3.68	3.17	0.794	2.16	9.19	25.6	1.62	22.0
11	10.00	3.68	3.17	0.794	2.16	9.19	25.3	1.62	21.6
12	10.00	3.30	2.85	0.724	2.09	7.52	23.0	1.33	19.8
13	10.00	3.30	2.85	0.724	2.09	7.52	22.8	1.33	19.4
14	10.00	3.30	2.85	0.772	2.14	7.52	22.4	1.42	18.7
15	10.00	3.67	3.16	0.858	2.23	9.29	24.9	1.76	20.8
16	10.00	3.68	3.17	1.128	2.65	12.23	27.3	2.32	20.9
17	10.00	3.68	3.17	0.747	2.12	9.17	26.3	1.53	23.0
18	10.00	3.68	3.17	0.747	2.12	9.17	26.0	1.53	22.6
19	10.00	3.68	3.17	0.845	2.21	9.17	24.8	1.73	21.0
20	10.00	3.68	3.17	0.845	2.21	9.17	24.6	1.73	20.6
21	10.00	3.30	2.85	0.684	2.05	7.54	23.6	1.26	20.5
22	10.00	4.24	3.66	0.865	2.23	12.26	30.2	2.05	26.3
23	10.00	3.20	2.86	0.704	1.80	7.97	23.3	1.46	19.3
24	10.00	3.30	2.86	0.261	1.36	3.00	19.9	0.55	19.0
25	10.00	2.80	2.50	0.464	1.56	4.62	19.0	0.84	16.7
26	10.00	2.90	2.50	0.194	1.29	1.97	17.3	0.36	16.7
27	10.00	2.50	2.22	0.904	2.00	7.92	21.7	1.44	14.9
28	10.00	2.55	2.22	0.329	1.42	2.92	16.2	0.54	14.6
29	10.00	2.93	2.50	0.230	1.33	2.37	17.5	0.43	15.5
30	10.00	2.93	2.50	0.350	1.45	3.64	18.3	0.66	16.7
31	10.00	2.96	2.50	0.160	1.25	1.63	17.1	0.30	14.5
32	10.00	2.95	2.50	0.230	1.33	2.37	17.8	0.43	15.5
33	10.00	2.94	2.50	0.230	1.33	2.37	17.2	0.44	15.3
34	10.00	2.95	2.50	0.240	1.34	2.37	17.0	0.46	16.2
35	10.00	2.95	2.50	0.220	1.32	2.37	18.0	0.41	17.3
36	10.00	3.04	2.50	0.250	1.34	2.37	17.2	0.43	16.3
37	10.00	3.22	2.50	0.270	1.36	2.37	17.0	0.43	16.3
38	10.00	3.92	3.33	0.170	1.27	2.37	22.6	0.43	22.2
39	10.00	2.35	2.00	0.290	1.38	2.37	14.7	0.43	13.4

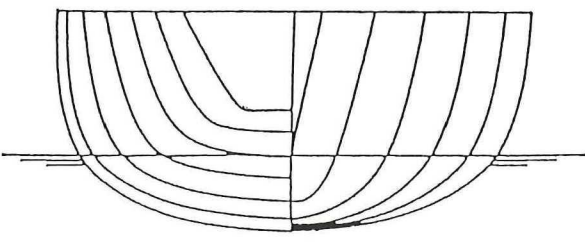
The parent body plans for models 1 - 22 and 29 - 39 are depicted in Figure 2. The waterline length of all models of

Series I (nrs. 1 - 22) is 1.60 meters; for the Series II and III (nrs. 23 - 28 and nrs. 29 - 39) the waterline length is 2.0 meters.

Table 3  
Form parameters

Model no.	$L_{WL}/B_{WL}$	$L_{WL}/B_{max}$	$B_{WL}/T_c$	$C_p$	$L_{WL}/v_c^{1/3}$	$L_{CA}$
1	3.17	2.73	3.99	0.568	4.78	-2.3
2	3.64	3.12	3.04	0.569	4.78	-2.3
3	2.76	2.35	5.35	0.565	4.78	-2.3
4	3.53	3.01	3.95	0.564	5.10	-2.3
5	2.76	2.36	3.96	0.574	4.36	-2.4
6	3.15	2.73	2.98	0.568	4.34	-2.4
7	3.17	2.72	4.95	0.562	5.14	-2.3
8	3.32	2.82	3.84	0.585	4.78	-2.4
9	3.07	2.62	4.13	0.546	4.78	-2.2
10	3.15	2.72	3.99	0.565	4.77	0.0
11	3.15	2.72	3.99	0.565	4.77	-5.0
12	3.51	3.03	3.94	0.565	5.10	0.0
13	3.51	3.03	3.94	0.565	5.10	-5.0
14	3.51	3.03	3.69	0.530	5.11	-2.3
15	3.16	2.72	3.68	0.530	4.76	-2.3
16	3.15	2.72	2.81	0.530	4.34	-2.3
17	3.15	2.72	4.24	0.600	4.78	0.0
18	3.15	2.72	4.24	0.600	4.78	-5.0
19	3.15	2.72	3.75	0.530	4.78	0.0
20	3.15	2.72	3.75	0.530	4.78	-5.0
21	3.51	3.03	4.17	0.600	5.10	-2.3
22	2.73	2.36	4.23	0.600	4.34	-2.3
23	3.50	3.13	4.06	0.548	5.00	-1.9
24	3.50	3.03	10.96	0.548	6.93	-2.1
25	4.00	3.57	5.39	0.548	6.01	-1.9
26	4.00	3.45	12.89	0.545	7.97	-2.1
27	4.50	4.00	2.46	0.548	5.02	-1.9
28	4.50	3.92	6.75	0.546	6.99	-1.9
29	4.00	3.41	10.87	0.549	7.50	-4.4
30	4.00	3.41	7.07	0.549	6.50	-4.4
31	4.00	3.30	15.82	0.549	8.50	-4.4
32	4.00	3.39	10.86	0.551	7.50	-2.1
33	4.00	3.40	10.87	0.545	7.50	-6.6
34	4.00	3.39	10.37	0.520	7.50	-4.4
35	4.00	3.39	11.47	0.579	7.50	-4.4
36	4.00	3.29	10.16	0.550	7.50	-4.3
37	4.00	3.11	9.45	0.551	7.50	-4.5
38	3.00	2.55	19.32	0.549	7.50	-4.4
39	5.00	4.26	6.96	0.549	7.50	-4.4

PARENT MODEL (nrs. 1 - 22)



PARENT MODEL (nrs. 23 - 39)

Fig. 2: Parent models for the Delft Systematic Yacht Hull Series.

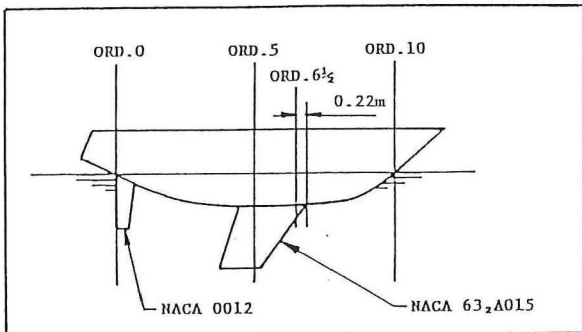
All models were tested with the same keel and rudder and consequently with the uniform extrapolation to  $L_{WL} = 10$  meters there is a difference in keel span for the Series I on the one hand and the Series II and III on the other hand.

For Series I the keel span is 1.37 meters and for Series II and III this is 1.10 meters for the corresponding waterline length  $L_{WL} = 10$  meters.

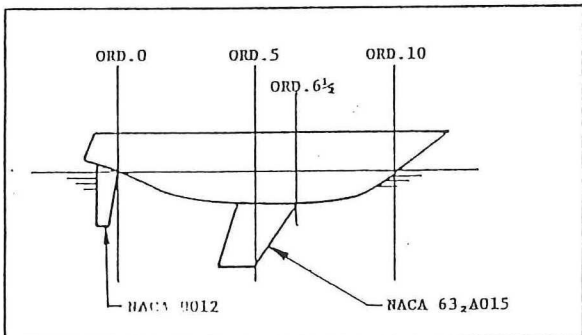
The keel and rudder location is given in Figure 3.

For the additional keel span variations of model 1 the following cases have been considered for the models 1a, 1b and 1c respectively: 1.25, 1.45 and 0.69 meters.

### MODELS 1 - 22



### MODELS 23 - 39



#### Geometry of keel and rudder

	volume m <sup>3</sup>	wetted area m <sup>2</sup>	rootchord m
Keel	0.00262	0.1539	0.414
Rudder	0.00023	0.0550	0.124

	tipchord m	span m	sweep back angle degrees
Keel	0.262	0.219	45
Rudder	0.096	0.266	5.4

Figure 3: Position of keel and rudder.

## 2.2. Determination of the hydrodynamic resistance

The total hydrodynamic resistance of a sailing yacht in calm water may be split up in three components:

$$R_\phi = R_T + R_i + R_H \quad (1)$$

Where:  $R_T$  - upright resistance (no leeway)

$R_i$  - induced resistance due to the generation of side force

$R_H$  - resistance due to heel (no side force)

### 2.2.1. Upright resistance

The upright resistance is split up in frictional resistance  $R_F$  and residuary resistance  $R_R$ .

The frictional resistance is calculated using the 1957 ITTC extrapolator:

$$C_F = \frac{0.075}{(\log R_n - 2)^2}, \quad R_n = \frac{VL}{\nu} \quad (2)$$

where the Reynolds number  $R_n$  for the hull is based on  $L = 0.7 L_{WL}$ . For keel and rudder the mean chord lengths have been used.

It has been considered to use the so called Prohaska form factors in the extrapolation procedure, but the difference in the final result is not significant.

For the analysis of the model experiment results the kinematic viscosity  $\nu$ , corresponding to the measured tank water temperature, has been used in all cases. For resistance prediction purposes:

$$\nu = 1.14 * 10^{-6} \text{ and } 1.19 * 10^{-6} \text{ m}^2 \text{ sec}^{-1}$$

for fresh water and seawater respectively at 15 degrees Celsius may be used.

The wetted surface of the canoe body, without keel and rudder can be approximated by:

$$S_C = [1.97 + 0.171 \frac{B_{WL}}{T_C}] * [\frac{0.65}{C_M}]^{1/3} * [\nabla_C * L_{WL}]^{1/2} \quad (3)$$

$$\text{with: } C_M = \frac{\nabla_C}{L_{WL} * B_{WL} * T_C * C_p}.$$

The frictional resistance follows from:

$$R_F = \frac{1}{2} \rho V^2 (S_C C_{Fc} + S_k C_{Fk} + S_r C_{Fr}) \quad (4)$$

where the indices c, k and r refer to respectively the canoe body, the keel and the rudder.

Using a least squares method the residuary resistance of all tested models is expressed in a polynomial expression,

using hull form parameters as variables. For the speed range  $F_n = 0.125$  (0.025) 0.450 the parameters  $C_p$ ,  $L_{WL}/V_C^{1/3}$ , LCB and  $B_{WL}/T_C$  have been used:

$$\begin{aligned} \frac{R_R}{\Delta_C} * 10^3 &= a_0 + a_1 C_p + a_2 (LCB) + a_3 (B_{WL}/T_C) + \\ &+ a_4 (L_{WL}/V_C^{1/3}) + a_5 C_p^2 + a_6 C_p * (L_{WL}/V_C^{1/3}) + \\ &+ a_7 (LCB)^2 + a_8 (L_{WL}/V_C^{1/3})^2 + a_9 (L_{WL}/V_C^{1/3})^3 \end{aligned} \quad (5)$$

For the speed range  $F_n = 0.475$  (0.025) 0.750 the polynomial fit is as follows:

$$\begin{aligned} \frac{R_R}{\Delta_C} * 10^3 &= c_0 + c_1 (L_{WL}/B_{WL}) + c_2 (A_w/V_C^{2/3}) + \\ &+ c_3 (LCB) + c_4 (L_{WL}/B_{WL})^2 + \\ &+ c_5 (L_{WL}/B_{WL}) * (A_w/V_C^{2/3})^3 \end{aligned} \quad (6)$$

The coefficients a and c are given in the Tables 4 and 5.

**Table 4**  
Residuary resistance polynomial coefficients

Fn	a0 a5	a1 a6	a2 a7	a3 a8	a4 a9
0.125	-6.735654 -38.86081	+38.36831 +0.956591	-0.008193 -0.002171	+0.055234 +0.272895	-1.997242 -0.017516
0.150	-0.382870 -39.55032	+38.17290 +1.219563	+0.007243 +0.000052	+0.026644 +0.824568	-5.295332 -0.047842
0.175	-1.503526 -31.91370	+24.40803 +2.216098	+0.012200 +0.000074	+0.067221 +0.244345	-2.448502 -0.015887
0.200	+11.292118 -11.41819	-14.51947 +5.654065	+0.047182 +0.007021	+0.085176 -0.094934	-2.673016 +0.006325
0.225	+22.17867 +7.167049	-49.16784 +8.600272	+0.085998 +0.012981	+0.150725 -0.327085	-2.878684 +0.018271
0.250	+25.90867 +24.12137	-74.75668 +10.48516	+0.153521 +0.025348	+0.188568 -0.854940	-0.889467 +0.048449
0.275	+40.97559 +53.01570	-114.2855 +13.02177	+0.207226 +0.035934	+0.250827 -0.715457	-3.072662 +0.039874
0.300	+45.83759 +132.2568	-184.7646 +10.06054	+0.357031 +0.066809	+0.338343 -1.719215	+3.871658 +0.095977
0.325	+89.20382 +331.1197	-393.0127 +8.598136	+0.617466 +0.104073	+0.460472 -2.815203	+11.54327 +0.155960
0.350	+212.6788 +667.6445	-801.7908 +12.39815	+1.087307 +0.166473	+0.538938 -3.026131	+10.80273 +0.165055
0.375	+336.2354 +831.1445	-1085.134 +26.18321	+1.644191 +0.238795	+0.532702 -2.450470	-1.224173 +0.139154
0.400	+566.5476 +1154.091	-1609.632 +51.46175	+2.016090 +0.288046	+0.265722 -0.178354	-29.24412 +0.018446
0.425	+743.4107 +937.4014	-1708.263 +115.6006	+2.435809 +0.365071	+0.013553 +1.838967	-81.16189 -0.062023
0.450	+1200.620 +1489.269	-2751.715 +196.3406	+3.208577 +0.528225	+0.254920 +1.379102	-132.0424 +0.013577

It should be noted that  $\Delta_C$  is the weight of displacement of the canoe body, without keel and rudder.  $V_C$  is the corresponding volume of displacement.

The waterplane area  $A_w$  may be approximated with sufficient accuracy by:

$$\begin{aligned} \frac{A_w}{L_{WL} * B_{WL}} &= 1.313C_p + 0.0371(L_{WL}/V_C^{1/3}) + \\ &- 0.0857C_p * (L_{WL}/V_C^{1/3}) \end{aligned} \quad (7)$$

**Table 5**  
Residuary resistance polynomial coefficients

Fn	c0	c1	c2	c3	c4	c5
.475	180.1004	-31.50257	-7.451141	2.195042	2.689623	0.006480
.500	243.9994	-44.52551	-11.15456	2.179046	3.857403	0.009676
.525	282.9873	-51.51953	-12.97310	2.274505	4.343662	0.011066
.550	313.4109	-56.58257	-14.41978	2.326117	4.690432	0.012147
.575	337.0038	-59.19029	-16.06975	2.419156	4.766793	0.014147
.600	356.4572	-62.85395	-16.85112	2.437056	5.078768	0.014980
.625	324.7357	-51.31252	-15.34595	2.334146	3.855360	0.013695
.650	301.1260	-39.79631	-15.02299	2.059657	2.545676	0.013588
.675	292.0571	-31.85303	-15.50548	1.847926	1.569917	0.014014
.700	284.4641	-25.14558	-16.15423	1.703981	0.817912	0.014575
.725	256.6367	-19.31922	-13.008450	2.152824	0.348305	0.011343
.750	304.1803	-30.11512	-15.85429	2.863173	1.524379	0.014031

## 2.2.2. Induced resistance

The induced resistance coefficient for a lifting surface with an effective aspect ratio  $AR_E$  is given by:

$$C_{Di} = \frac{C_L^2}{\pi AR_E} \quad (8)$$

Similarly, for the hull, keel and rudder combination, the induced resistance resulting from the generated sideforce  $F_H$  can be written as:

$$R_i = \frac{1}{\pi AR_E} * \frac{F_H^2}{qS_C} \quad (9)$$

where  $AR_E$  is the effective aspect ratio of the hull, keel and rudder combination, and  $q = \frac{1}{2}\rho V^2$ . Using the results of the resistance measurements with heel angle and leeway, the induced resistance could be expressed by:

$$R_i = (C_0 + C_2 \varphi^2) \frac{F_H^2}{qS_C} \quad (10)$$

where  $C_0$  and  $C_2$  depend on the geometry of the hull, keel and rudder combination.

The expression (10) works well for Series I (nrs. 1 - 22) but for the Series II and III (nrs. 23 - 39) an additional term with the Froude number  $F_n$  was necessary to cope with a significant free surface influence on the induced resistance. Thus:

$$R_i = (C_0 + C_2 \varphi^2 + C_3 F_n) \frac{F_H^2}{qS_C} \quad (11)$$

For Series I a fair agreement between (10) and (11) exists for  $F_n = 0.325$ . With (9) and (10) we find:

$$AR_E = \frac{1}{\pi (C_0 + C_2 \varphi^2)} \quad (12)$$

We now define an effective draught  $T_E$  with:

$$AR_E = \frac{T_E^2}{S_C} , \text{ than:}$$

$$T_E^2 = \frac{S_C}{\pi (C_0 + C_2 \varphi^2)} \quad (13)$$

and:

$$R_i = \frac{F_H^2}{\pi T_E^2 q} \quad (14)$$

With the measured  $F_H$  values for models 1 - 28 and model 1a, model 1b and model 1c the effective draughts  $T_E$  have been determined for heel angles 0, 10, 20 and 30 degrees.

The relative effective draught  $T_E/T$  appears to be strongly dependent on  $T_C/T$ ,  $B_{WL}/T_C$  and  $\varphi$ .

A satisfactory fit to the experimental data is given by:

$$\frac{T_E}{T} = A_1 \left( \frac{T_C}{T} \right) + A_2 \left( \frac{T_C}{T} \right)^2 + A_3 \left( \frac{B_{WL}}{T_C} \right) \quad (15)$$

$$\text{with: } A_1 = 4.080 + 0.0370 \varphi - 4.9830 \varphi^3$$

$$A_2 = -4.179 - 0.8090 \varphi + 9.9670 \varphi^3$$

$$A_3 = 0.055 - 0.0339 \varphi - 0.0522 \varphi^3$$

$\varphi$  in radians.

### 2.2.3. Resistance due to heel

For each of the models 1 - 28 the resistance due to heel,  $R_H$ , has been determined.

It was found that a reasonable approximation of  $R_H$  is given by:

$$\frac{R_H}{qS_C} = C_H F_n^2 \varphi \quad (16)$$

$\varphi$  in radians.

The  $C_H$  was expressed in the keel and hull parameters  $T_C/T$  and  $B_{WL}/T_C$ .

$$C_H * 10^3 = 6.747 \left( \frac{T_C}{T} \right) + 2.517 \left( \frac{B_{WL}}{T_C} \right) + 3.710 \left( \frac{B_{WL}}{T_C} \right) * \left( \frac{T_C}{T} \right) \quad (17)$$

The resistance due to heel and side force, the heeled resistance, is given by:

$$R_i + R_H = \frac{F_H^2}{\pi T_E^2 q} + (C_H F_n^2 \varphi) q S_C \quad (18)$$

with  $T_E$  and  $C_H$  as shown in (15) and (17)

For  $\varphi > 30$  degrees an extra resistance increase can be included to allow for

the influence of deck immersion.

By analogy with the IMS formulation the following expression is used for velocity predictions:

$$R_\varphi = R_{\varphi 0} [1 + 0.0004 (\varphi - 30)^2] \quad (19)$$

$\varphi$  in degrees.

This results in a resistance increase of 1% and 4% for respectively  $\varphi = 35$  degrees and  $\varphi = 40$  degrees.

### 2.3. Side force as a function of heel and leeway

For the models 1 - 22 (Series I) and model 1c (half keel span) the relation between leeway and side force is approximated by:

$$\beta = \frac{F_H \cos \varphi}{q S_C} (B_0 + B_2 \varphi^2) \quad (20)$$

$\beta$  and  $\varphi$  in radians

Due to larger  $B_{WL}/T_C$  an additional term depending of the heel angle and the Froude number is necessary for the models 23 - 28 (Series II) to satisfy the experimental evidence which indicates free surface effects.

Thus:

$$\beta = \frac{F_H \cos \varphi}{q S_C} (B_0 + B_2 \varphi^2) + B_3 \varphi^2 F_n \quad (21)$$

If the combination of hull, keel and rudder is considered as a side force (lift) generating element, the "lift" slope will be given by the first two terms of (21):

$$\frac{F_H \cos \varphi}{\beta q S_C} = \frac{1}{B_0 + B_2 \varphi^2} \quad (22)$$

The slope depends on the effective aspect ratio of the underwater part of the hull, keel and rudder, which in this case is related to side force generation.

It was found that the "lift" slope can be expressed with sufficient accuracy by:  $T_C/T$  and  $T^2/S_C$ :

$$\frac{F_H \cos \varphi}{\beta q S_C} = b_1 \left( \frac{T^2}{S_C} \right) + b_2 \left( \frac{T^2}{S_C} \right)^2 + b_3 \left( \frac{T_C}{T} \right) + b_4 \left( \frac{T_C}{T} \right) * \left( \frac{T^2}{S_C} \right) \quad (23)$$

with:

	$\varphi = 0^\circ$	$\varphi = 10^\circ$	$\varphi = 20^\circ$	$\varphi = 30^\circ$
b <sub>1</sub>	+ 2.025	+ 1.989	+ 1.980	+ 1.762
b <sub>2</sub>	+ 9.551	+ 6.729	+ 0.633	- 4.957
b <sub>3</sub>	+ 0.631	+ 0.494	+ 0.194	- 0.087
b <sub>4</sub>	- 6.575	- 4.745	- 0.792	+ 2.766

The coefficient  $B_3$  in (21) has been determined with the experimental results of models 23 - 28 (Series II):

$$B_3 = 0.0092 \left( \frac{B_{WL}}{T_C} \right) * \left( \frac{T}{T_C} \right) \quad (24)$$

The contribution of the  $B_3$  is relatively small, except in the case of very large  $B_{WL}/T_C$  and  $T/T_C$ , such as models 24 and 26. Then there is a certain heel angle at which no side force is generated, which follows from:

$$\beta = B_3 \varphi^2 F_n.$$

#### 2.4. Stability

The data reduction of the experimental stability data has been carried out as follows (see Figure 4):

$$GN \sin \varphi = GM \sin \varphi + MN \sin \varphi \quad (25)$$

where  $GM$  is the calculated hydrostatic value at  $V = 0$ . The residual stability lever can be expressed in:  $\varphi$ ,  $F_n$  and  $B_{WL}/T_C$ :

$$\frac{MN \sin \varphi}{L_{WL}} = (D_2 * \varphi * F_n + D_3 \varphi^2) \quad (26)$$

with:

$$D_2 = -0.0406 + 0.0109 \left( \frac{B_{WL}}{T_C} \right) - 0.00105 \left( \frac{B_{WL}}{T_C} \right)^2$$

$$D_3 = + 0.0636 - 0.0196 \left( \frac{B_{WL}}{T_C} \right)$$

$\varphi$  in radians

Finally the distance of the center of lateral resistance to the waterline is given by:

$$D_4 * T \quad (27)$$

with:

$$D_4 = 0.414 - 0.165 \left( \frac{T_C}{T} \right)$$

Apparently for  $T_C/T \rightarrow 0$   $D_4$  approaches the value for an elliptic distribution of the sideforce from the tip of the keel to the waterline.

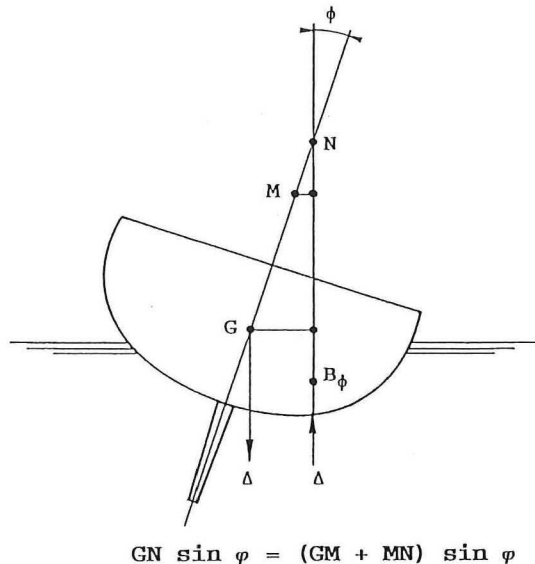


Fig. 4: Definition of residual stability lever  $MN \sin \varphi$ .

To show the goodness of fit of the various polynomials as given for resistance, side force, and stability, some results are given in the Figures 5 - 8.

In Figure 5 the measured and predicted up-right resistance for the models 16 and 37 (a heavy- and light-displacement hull) are compared. The typical difference in character of the resistance curve for speeds excluding  $F_n = 0.45$  is clearly shown.

In Figure 6 the heeled resistance, predicted with equation (18) is compared with the experimental results for models 16 and 28, and in Figure 7 the generated side force as a function of leeway and heel angle predicted according to equation (21) is compared with the measurements.

Finally a similar comparison has been made for the stability lever at 10, 20 and 30 degrees as a function of the Froude number using equations (25) and (26).

The examples include some rather extreme hull forms, but the prediction in all considered cases is satisfactory. The importance of the length-displacement ratio  $L_{WL}/v_C^{1/3}$  and the beam to draught ratio  $B_{WL}/T_C$  is clearly shown in the Figures 5 - 8.

In particular the attention is drawn to the loss of stability at forward speed for the wide beam models 31 and 33 as depicted in Figure 8.

#### 3. Prediction of added resistance in waves

To estimate the added resistance in waves the radiated damping energy of the vertical motions (heave and pitch) is related to the work done by the extra resistance  $R_{AW}$ , as described in [7]:

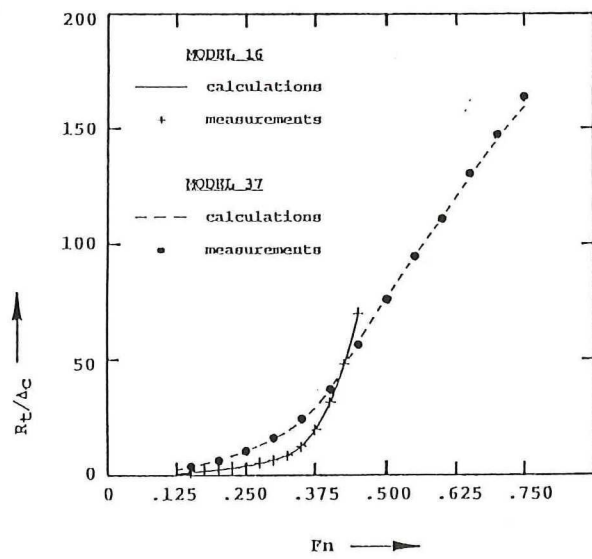


Fig. 5: Measured and predicted upright resistance.

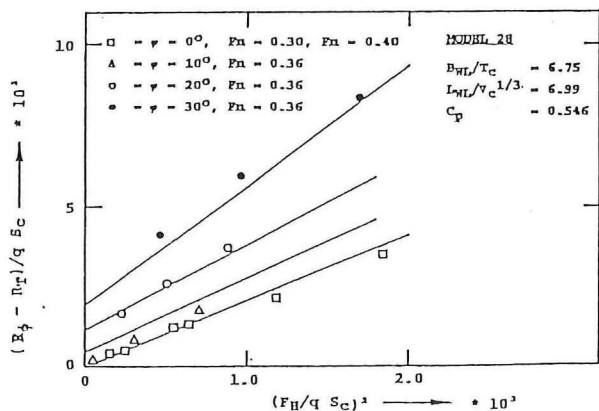
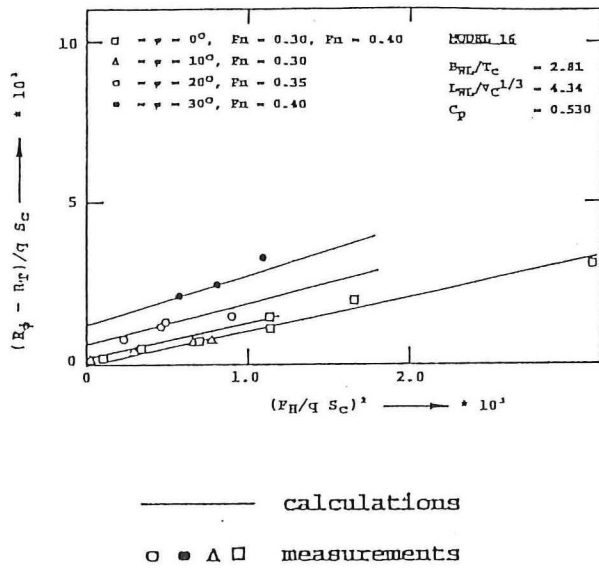


Fig. 6: Measured and predicted heeled resistance.

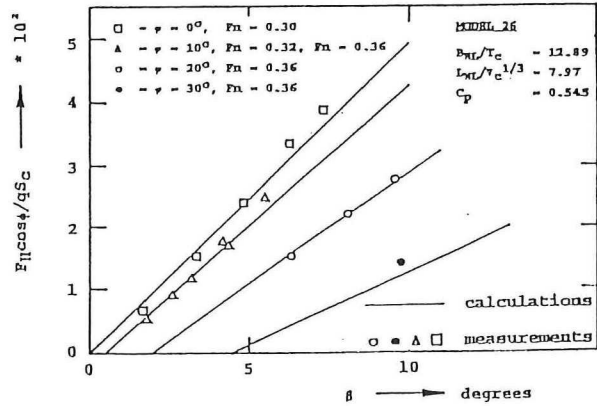
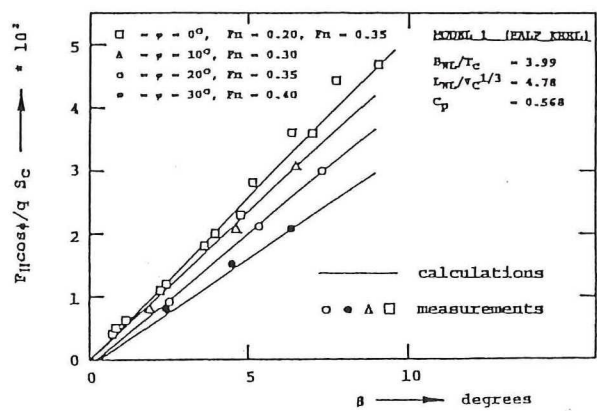


Fig. 7: Measured and predicted side-force.

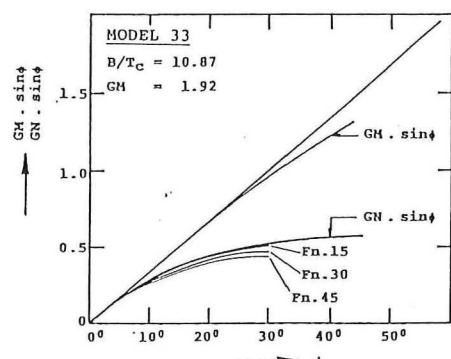
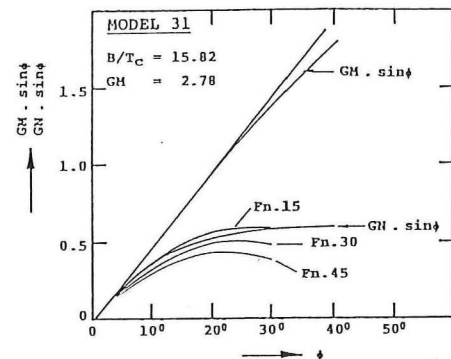


Fig. 8: Stability lever GN sin φ as a function of Fn. The measured values for Fn = .15, .30 and .45 coincide with the drawn lines.

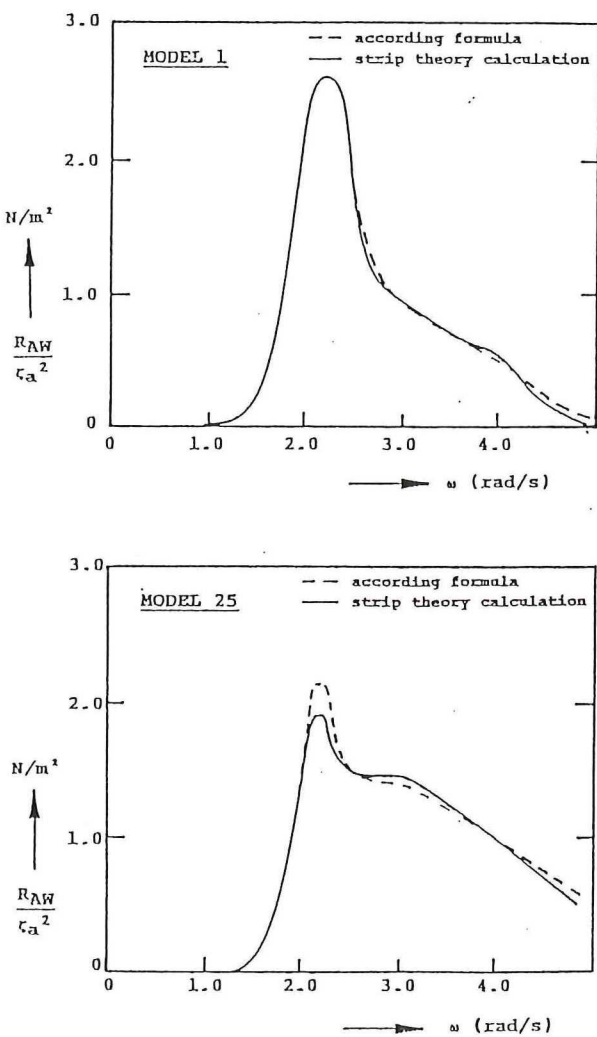


Fig. 9: Added resistance operators for models 1 and 25.

$$R_{AW} = \frac{1}{\lambda} \int_0^{L_{WL}} \int_0^{T_e} b' V_z^2 dx_b dt \quad (28)$$

where:

- $\lambda$  - wave length
- $t$  - time
- $b'$  - cross sectional damping coefficient, corrected for the forward speed
- $V_z$  - relative vertical velocity of the considered cross-section with respect to the water.
- $T_e$  - period of wave encounter
- $x_b$  - length ordinate of the hull.

The vertical relative motion  $V_z$  depends on the vertical motions heave and pitch and the vertical component of the incident wave velocity. The calculation of  $V_z$  can be carried out by a simple strip theory, ignoring 3-dimensional effects.

As shown in [7] and [9] calculated added resistance in general agrees quite well with the results of model resistance experiments in regular waves. It is shown that the added resistance is proportional to the wave height squared for constant wave-length and forward speed. The added resistance on a base of wavelength or wave period for a certain yacht speed (preferably in dimensionless quantities) is the added wave resistance response operator.

In combination with a given wave spectrum  $S_\zeta$ , which could be the result of a wave buoy measurement, or a formulation based on observed wave period and significant wave height, the mean added resistance in the considered wave spectrum can be obtained by superposition:

$$\bar{R}_{AW} = 2 \int_0^\infty \frac{R_{AW}}{\zeta a^2} * S_\zeta(\omega_e) d\omega_e \quad (29)$$

In general the added resistance operator  $R_{AW}/\zeta a^2$  or a corresponding dimensionless presentation, depends on the hull geometry, the longitudinal pitch gyroradius, the wave period or frequency and the wave direction  $\mu_w$ .

For eight models of the Delft Systematic Yacht Hull Series, nrs: 1, 5, 6, 22, 25, 26, 30 and 31, which constitute a very large range of hull form variations, the added resistance response operators have been calculated for wave directions  $\mu_w = 100, 115, 125$  and  $135$  degrees, forward speeds corresponding to  $F_n = 0.15 (0.10)$   $0.45$  and  $0.60$  and pitch gyroradius  $k_{yy}/L_{WL} = 0.25, 0.27$ , and  $0.31$ .

The calculations concern the upright conditions. Based on the model tests in [7] this is a reasonable estimate also for conditions when heeled.

The added resistance operators have been used to estimate the mean added resistance in a Bretschneider spectrum defined by the significant wave height  $\bar{H}_{1/3}$  and the mean wave period  $\bar{T}_1$ :

$$S_\zeta = A \omega^{-5} \exp(-B \omega^{-4}) \quad (30)$$

with:  $A = 173 \bar{H}_{1/3}/\bar{T}_1^4$  and  $B = 691/\bar{T}_1^4$

Using equation (29) the mean added resistance  $\bar{R}_{AW}$  has been calculated for  $\bar{H}_{1/3} = 1$  meter,  $\bar{T}_1 = 2$  (0.5) 6 seconds and the same wave directions as for the regular wave case, assuming unidirectional waves.

In particular the gyroradius range is very wide, and presumably exceeds the practical possibilities. For significant wave heights differing from  $\bar{H}_{1/3} = 1$  meter the added resistance has to be multiplied by the square of the considered wave height.

A systematic analysis of the results of this calculation showed that for constant wave direction, wave height, wave period and forward speed the added

resistance depends for the greater part on:

$$v_c^{1/3}/L_{WL} * k_{YY}/L_{WL}$$

See Figure 10 for  $\bar{T}_1 = 4$  seconds,  $\bar{H}_{1/3} = 1.50$  meters,  $F_n = 0.35$  and  $L_{WL} = 10$  meters, as an example.

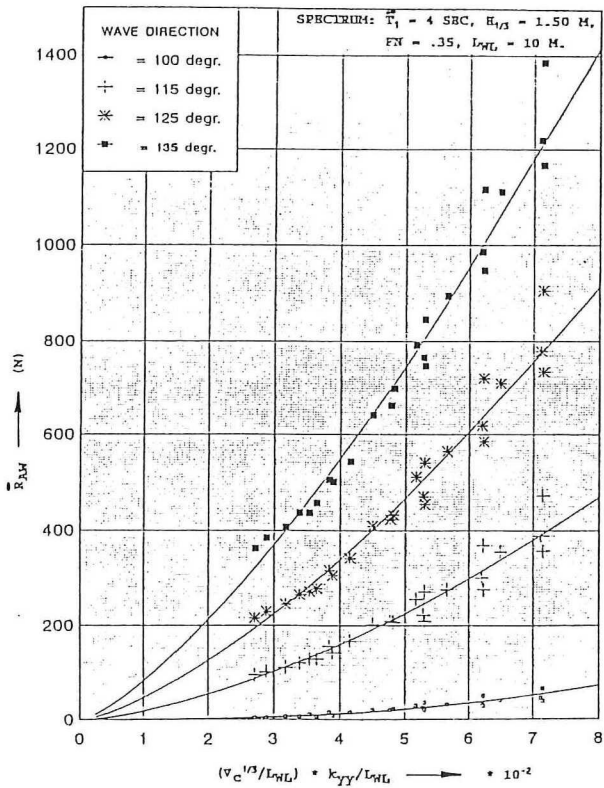


Fig. 10: Added resistance.

The data may be used to analyse the influence of the pitch gyroradius on the added resistance. Also, as an example, this is shown in Figure 11a where  $\bar{R}_{AW}$  is plotted on a base of  $\bar{T}_1$  for model no. 1 with  $L_{WL} = 10$  meters and gyroradii  $k_{YY}/L_{WL} = 0.23, 0.27$  and  $0.31$ .

A similar picture is given in Figure 11b for model no 26, the parent model of the light-displacement models.

The total result of this added resistance calculation in dimensionless form can be summarized by:

$$\frac{\bar{R}_{AW} * 10^2}{\rho g L_{WL} \bar{H}_{1/3}^2} = a \left[ 10^2 * \frac{v_c^{1/3}}{L_{WL}} * \frac{k_{YY}}{L_{WL}} \right]^b \quad (31)$$

where  $a$  and  $b$  are given in Table 7. The goodness of fit is shown in the Figure 12a, b for  $\bar{T}_1 = 2.476$  and  $4.457$  seconds and  $F_n = 0.3$ . This set of data have been used in the Delft Velocity Prediction Program to estimate the yacht speed in a given wave condition. The extra input is no more than the significant wave height  $\bar{H}_{1/3}$ , the wave period  $\bar{T}_1$  and the pitch gyroradius of the considered yacht.

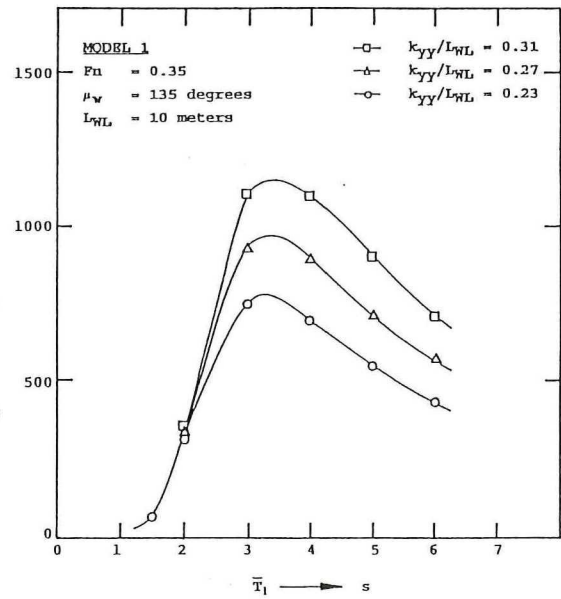


Figure 11a: Added resistance versus mean wave period Model No. 1.

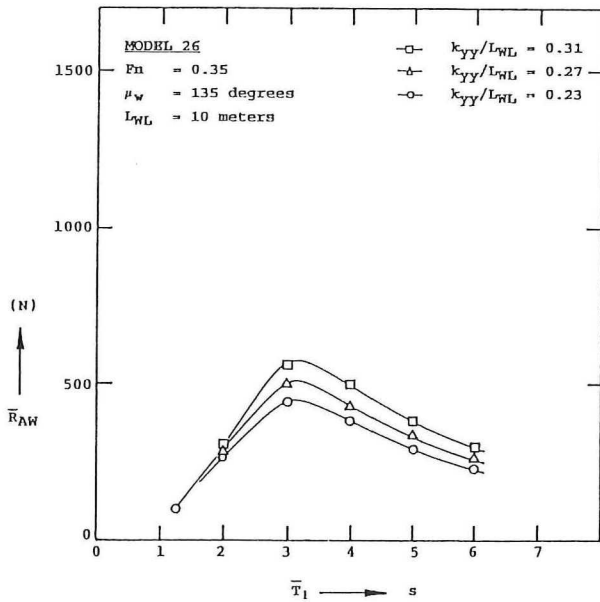


Figure 11b: Added resistance versus mean wave period Model No. 26.

It should be noted that the analysis is restricted to wave directions forward of the beam. For waves aft of the beam the calculation of the extra resistance in a given wave spectrum according to the strip theory is not reliable. However, in general, the added resistance in this region is relatively small. Also, effects of surfing are not included.

Table 7 Added resistance coefficients a and b (see equation (31))					.25	3.467	125	0.027	1.424
Fn	$\bar{T}_l \sqrt{(g/L_{WL})}$	$\mu_w$	a	b	.25	3.467	115	0.010	1.580
.15	1.981	135	0.649	0.440	.25	3.467	100	0.00011	2.949
.15	1.981	125	0.352	0.593	.25	3.467	135	0.028	1.418
.15	1.981	115	0.127	0.841	.25	3.467	125	0.015	1.483
.15	1.981	100	0.0011	2.455	.25	3.467	115	0.006	1.636
.15	2.476	135	0.209	0.904	.25	4.457	100	0.00006	3.053
.15	2.476	125	0.114	1.027	.25	4.457	135	0.017	1.456
.15	2.476	115	0.040	1.247	.25	4.457	125	0.009	1.519
.15	2.476	100	0.00032	2.863	.25	4.457	115	0.004	1.663
.15	2.971	135	0.089	1.124	.25	4.952	100	0.00005	2.905
.15	2.971	125	0.048	1.229	.25	4.952	135	0.011	1.482
.15	2.971	115	0.017	1.437	.25	4.952	125	0.006	1.540
.15	2.971	100	0.00014	3.005	.25	4.952	115	0.0023	1.686
.15	3.467	135	0.045	1.232	.25	5.447	100	0.00005	2.675
.15	3.467	125	0.024	1.329	.25	5.447	135	0.007	1.501
.15	3.467	115	0.008	1.532	.25	5.447	125	0.004	1.548
.15	3.467	100	0.00004	3.391	.25	5.447	115	0.0015	1.707
.15	3.962	135	0.026	1.293	.25	5.943	100	0.0011	1.692
.15	3.962	125	0.014	1.385	.25	5.943	135	0.0010	1.000
.15	3.962	115	0.005	1.590	Fn	$\bar{T}_l \sqrt{(g/L_{WL})}$	$\mu_w$	a	b
.15	3.962	100	0.00003	3.259	.15	1.981	135	0.843	0.241
.15	4.457	135	0.016	1.329	.15	1.981	125	0.487	0.435
.15	4.457	125	0.008	1.417	.15	1.981	115	0.195	0.710
.15	4.457	115	0.003	1.601	.15	1.981	100	0.004	1.929
.15	4.457	100	0.00004	2.863	.15	2.476	135	0.283	0.856
.15	4.952	135	0.010	1.345	.15	2.476	125	0.162	0.984
.15	4.952	125	0.005	1.428	.15	2.476	115	0.065	1.182
.15	4.952	115	0.0019	1.617	.15	2.476	100	0.0012	2.283
.15	4.952	100	0.00004	2.618	.15	2.476	135	0.014	1.146
.15	5.447	135	0.007	1.364	.15	2.476	125	0.071	1.235
.15	5.447	125	0.004	1.445	.15	2.476	115	0.028	1.396
.15	5.447	115	0.0012	1.650	.15	2.476	100	0.0005	2.445
.15	5.447	100	0.00004	2.414	.15	3.467	135	0.064	1.289
.15	5.943	135	0.005	1.371	.15	3.467	125	0.036	1.362
.15	5.943	125	0.003	1.441	.15	3.467	115	0.014	1.504
.15	5.943	115	0.0009	1.643	.15	3.467	100	0.00027	2.519
.15	5.943	100	0.00005	2.220	.15	3.962	135	0.037	1.367
.15					.15	3.962	125	0.021	1.430
.15					.15	3.962	115	0.008	1.558
Fn	$\bar{T}_l \sqrt{(g/L_{WL})}$	$\mu_w$	a	b	.25	3.962	100	0.00016	2.548
.25	1.981	135	0.669	0.416	.35	4.457	135	0.023	1.411
.25	1.981	125	0.380	0.583	.35	4.457	125	0.013	1.465
.25	1.981	115	0.148	0.832	.35	4.457	100	0.00008	2.691
.25	1.981	100	0.0021	2.195	.35	4.952	135	0.015	1.439
.25	2.476	135	0.219	0.963	.35	4.952	125	0.008	1.493
.25	2.476	125	0.124	1.078	.35	4.952	115	0.003	1.599
.25	2.476	115	0.048	1.275	.35	4.952	100	0.00005	2.557
.25	2.476	100	0.0007	2.565	.35	5.447	135	0.010	1.448
.25	2.971	135	0.095	1.221	.35	5.447	125	0.006	1.513
.25	2.971	125	0.053	1.308	.35	5.447	115	0.0022	1.637
.25	2.971	115	0.020	1.478	.35	5.447	100	0.00007	2.293
.25	2.971	100	0.00025	2.789	.35	5.943	135	0.007	1.462
.25	3.467	135	0.048	1.349	.35	5.943	125	0.004	1.513

.35	5.943	115	0.0015	1.631	.60	3.467	100	0.0010	1.871
.35	5.943	100	0.00006	2.228	.60	3.962	135	0.071	1.087
Fn	$\bar{T}_1 \sqrt{g/L_{WL}}$	$\mu_w$	a	b	.60	3.962	125	0.041	1.148
					.60	3.962	115	0.0017	1.258
					.60	3.962	100	0.00056	1.929
.45	1.981	135	1.117	0.004	.60	4.457	135	0.044	1.134
.45	1.981	125	0.647	0.232	.60	4.457	125	0.026	1.189
.45	1.981	115	0.262	0.543	.60	4.457	115	0.0107	1.286
.45	1.981	100	0.006	1.657	.60	4.457	100	0.00034	1.891
.45	2.476	135	0.376	0.693	.60	4.952	135	0.029	1.163
.45	2.476	125	0.217	0.840	.60	4.952	125	0.017	1.210
.45	2.476	115	0.088	1.050	.60	4.952	115	0.007	1.308
.45	2.476	100	0.0022	2.005	.60	4.952	100	0.00027	1.837
.45	2.971	135	0.166	1.016	.60	5.447	135	0.020	1.176
.45	2.971	125	0.096	1.115	.60	5.447	125	0.012	1.222
.45	2.971	115	0.039	1.272	.60	5.447	115	0.005	1.323
.45	2.971	100	0.0009	2.173	.60	5.447	100	0.00013	2.046
.45	3.467	135	0.086	1.172	.60	5.943	135	0.014	1.187
.45	3.467	125	0.050	1.247	.60	5.943	125	0.008	1.238
.45	3.467	115	0.020	1.382	.60	5.943	115	0.0034	1.315
.45	3.467	100	0.0005	2.232	.60	5.943	100	0.00011	1.921
.45	3.962	135	0.050	1.254					
.45	3.962	125	0.029	1.317					
.45	3.962	115	0.012	1.436					
.45	3.962	100	0.00029	2.247					
.45	4.457	135	0.031	1.302					
.45	4.457	125	0.018	1.356					
.45	4.457	115	0.007	1.476					
.45	4.457	100	0.00020	2.196					
.45	4.952	135	0.020	1.327					
.45	4.952	125	0.011	1.382					
.45	4.952	115	0.0046	1.494					
.45	4.952	100	0.00008	2.498					
.45	5.447	135	0.014	1.347					
.45	5.447	125	0.008	1.399					
.45	5.447	115	0.003	1.508					
.45	5.447	100	0.00008	2.318					
.45	5.943	135	0.010	1.358					
.45	5.943	125	0.006	1.405					
.45	5.943	115	0.0022	1.514					
.45	5.943	100	0.00011	1.896					

Fn	$\bar{T}_1 \sqrt{g/L_{WL}}$	$\mu_w$	a	b
.60	1.981	135	1.677	-0.386
.60	1.981	125	0.975	-0.109
.60	1.981	115	0.394	0.263
.60	1.981	100	0.013	1.294
.60	2.476	135	0.552	0.421
.60	2.476	125	0.315	0.603
.60	2.476	115	0.129	0.842
.60	2.476	100	0.004	1.641
.60	2.971	135	0.235	0.811
.60	2.971	125	0.137	0.925
.60	2.971	115	0.057	1.087
.60	2.971	100	0.0020	1.790
.60	3.467	135	0.122	0.995
.60	3.467	125	0.071	1.076
.60	3.467	115	0.030	1.201

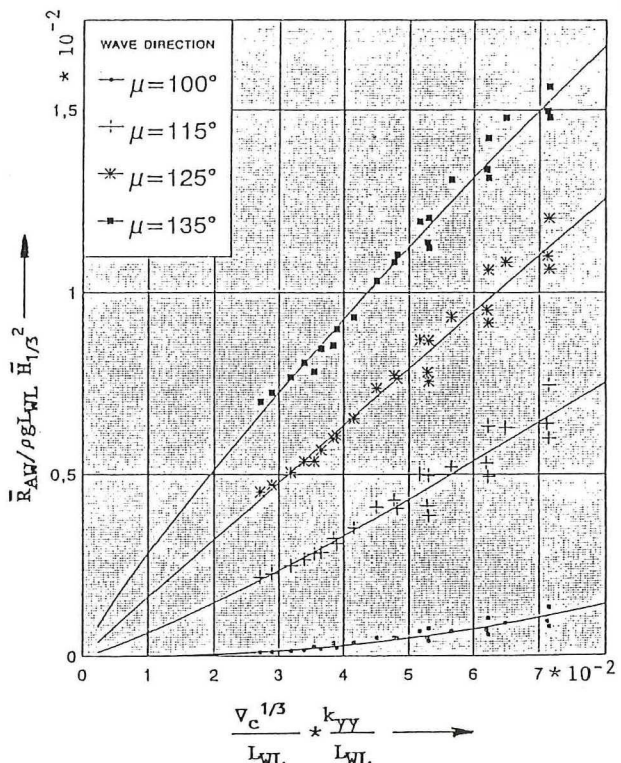


Fig. 12a: Mean added wave resistance for  $\bar{T}_1 \sqrt{g/L_{WL}} = 2.475$  and  $Fn = 0.35$

When measured wave spectra are available a different approach to the estimation of the added resistance in waves is required.

In this case the added resistance response operator of the considered yacht has to be known.

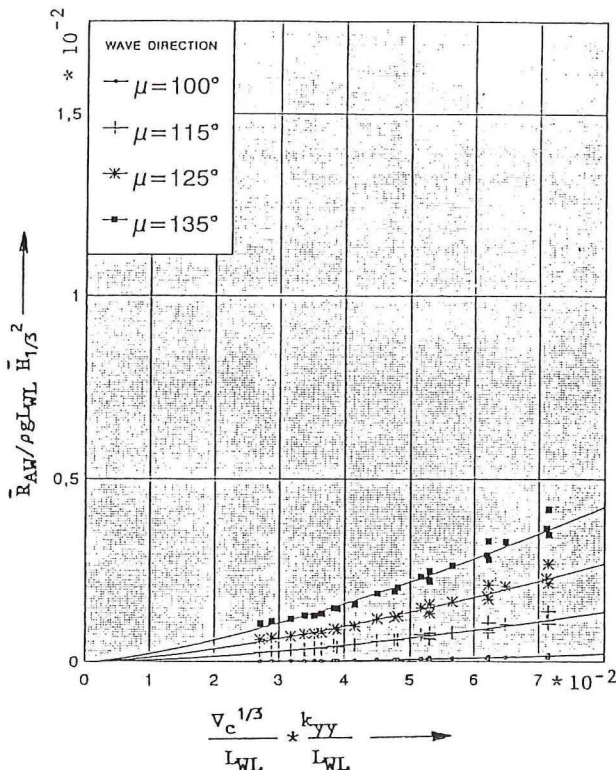


Fig. 12b: Mean added wave resistance for  $T_1 \sqrt{g/L_{WL}} = 4.457$  and  $Fn = 0.35$

With the computational capacity of today's personal computers the added resistance response operator of a yacht can be easily determined when the lines-plan and the longitudinal distribution of mass are given as shown in [7] and [9]. The mean added resistance then follows from equation (29).

Another approach for this case, by Reumer [3], uses an approximation of the added resistance response operator. For all 39 models of the Delft Systematic Series the operator has been calculated for a range of Froude numbers, wave frequencies, wave directions and pitch gyroradii.

Using a least squares procedure the resulting added resistance operators could be expressed in one polynomial expression:

$$\frac{R_{AW}}{\zeta a^2} = a_1(L_{WL}/v_C^{1/3}) + a_2(L_{WL}/v_C^{1/3})^2 + \\ + a_3(L_{WL}/v_C^{1/3})^3 + a_4(L_{WL}/B_{WL}) + \\ + a_5(L_{WL}/B_{WL})^2 + a_6(B_{WL}/T_C) + \\ + a_7 C_p + a_8 C_p^2 + a_9 C_p^3 \quad (32)$$

The coefficients  $a_1$  to  $a_9$  are a function of the wave direction, wave frequency and the Froude number.

In Fig. 9 the result of (32) is compared with a direct computation for the models 1 and 25, assuming a waterline length  $L_{WL} = 10$  meters,  $\mu_w = 165$  degrees (15 degrees off the bow) and  $Fn = 0.25$ .

The methods described above may be used to analyse the relative importance of the mean added resistance of a sailing yacht in a seaway by including the calculated  $R_{AW}$  in a velocity prediction.

#### 4. References

- [1] Gerritsma, J. and J.A. Keuning, Performance of light- and heavy displacement sailing yachts in waves, The Second Tampa Bay Sailing Yacht Symposium, St. Petersburg, Florida 1988.
- [2] Monhaupt, A., ITC, Comparative study of different polynomial formulations for the residuary resistance of the Systematic Delft Series model 1 to 28.
- [3] Reumer, J.G., Een ontwerp voor een eenvoudige polynoombenadering van de toegevoegde weerstand van zeiljachten in golven, Technische Universiteit Delft Afstudeerwerk, Rapportnr. 874-S, 1991.
- [4] Gerritsma, J. and G. Moeyes, The seakeeping performance and steering properties of sailing yachts, 3rd HISWA Symposium 1973, Amsterdam.
- [5] Gerritsma, J., G. Moeyes and R. Onnink, Test results of a systematic yacht hull series, 5th HISWA Symposium, 1977, Amsterdam.
- [6] Gerritsma, J., R. Onnink and A. Versluis, Geometry, resistance and stability of the Delft Systematic Yacht Hull Series, 7th HISWA Symp., 1981, Amsterdam.
- [7] Gerritsma, J. and J.A. Keuning, Performance of light- and heavy displacement sailing yachts in waves, 2nd Tampa Bay Sailing Yacht Symposium, 1988, St. Petersburg, Florida.
- [8] Gerritsma, J., J.A. Keuning and R. Onnink, The Delft Systematic Yacht Hull Series II experiments, 10 th Chesapeake Sailing Yacht Symposium, 1991, Annapolis.
- [9] Gerritsma, J. and W. Beukelman, Analysis of the resistance increase in waves of a fast cargo ship, International Shipbuilding Progress, Vol.19, Nr. 217, 1972.